Ocean Engineering 153 (2018) 53–59

Contents lists available at ScienceDirect

Ocean Engineering

journal homepage: www.elsevier.com/locate/oceaneng

Water entry of a constraint posture body under different entry angles and ventilation rates

Yunhua Jiang [a,*], Tao Bai [b], Ye Gao [a], Lianwu Guan [b]

[a] Department of Aerospace Engineering, Harbin Engineering University, Harbin, Heilongjiang, 150001, PR China
[b] College of Automation, Harbin Engineering University, Harbin, Heilongjiang, 150001, PR China

ARTICLE INFO

Keywords:
Constraint posture projectile
Water entry
Ventilation cavity
Multiphase flow

ABSTRACT

Water entry experiments of a constraint posture projectile were performed under different entry angles and ventilation rates. The near water surface cavity flow characteristics, including splash sheet, surface closure, pull away, deep closure and cavity ripples, were investigated under different entry angles and ventilation rates without the posture perturbation influence of the projectile. The experimental results demonstrate that, the dimensionless cavity surface closure and pull away time increase gradually with the increasing of the water entry angle, and the dimensionless cavity deep closure time and the pinch off depth experience a slight increase and decrease, respectively. The deep closure patterns shift from the point closure to the line closure as the water entry angle increases for the oblique water entry cases. And, the cavity ripples were observed before the pinch off and after the pull away for ours experiment, which are more likely acoustic in origin. In addition, the surface closure contributed by the splash sheet is clearly delayed at similar entry conditions except for the ventilation rate. The dimensionless cavity deep closure times of the ventilation cases are significantly higher than the cases without ventilation. However, with further increase the ventilation, the deep closure time changes slightly.

1. Introduction

Water entry is a fundamental problem widely presents in different applications, which including some natural phenomena such as a basilisk lizard walking on the water surface (Glasheen and Mcmahon, 1996) and a stone skipping on water (Clanet et al., 2004), military application such as antitorpedo and antisubmarine water entry (May 1975), aerospace engineering such as aerospace structures water entry impaction (Seddon and Moatamedi, 2016), and even the sports such as the water entry of swimmers and divers, and the entry and exit of the oars in rowing (Truscott et al., 2012). There are three mainly science problems for object water entry, as follows: the prediction of the impaction load, the calculation of the vehicle trajectory with the cavity running, and the understanding of the air cavity development.

In the present study, we focus on investigating experimentally the effects of the entry angle and ventilation rate to the air entraining cavity development, which are the most typical operating situation for antitorpedo and antisubmarine water entry (May, 1975), aerospace structures water entry impaction (Seddon and Moatamedi, 2016), and supercavitating vehicle water entry (Semenenko, 2001). Specifically, water entry experiments of a constraint posture projectile were conducted for understanding the fundamental flow characteristics involved in oblique and ventilation water entry.

In general, there are typical flow phenomena including the crown splash, surface closure, pull away, deep closure and cavity ripples in the water entry experiments, which were systematically investigated with a sphere under different entry velocities and surface treatments (Worthington and Cole, 1897; Truscott et al., 2014; Marston et al., 2016). Specifically, for the crown splash, the earliest images were captured by Worthington and Cole (1897), in which the splash sheet water is coming from the undisturbed water surface layer and no additional water contribution to it after its formation. After that, the crown splash has been presented with extensive high-speed imaging studies (Bell, 1924; Logvinovich, 1973; May, 1975; Duez et al., 2007). Recently, the crown splash buckling-type azimuthal instability structure were captured in Marston et al. (2016), i.e. the instability is structured by vertical striations along the crown and a thin film connects each striation. After crown splash buckling-type azimuthal instability, the surface closure appears, which means the flow into the cavity is completely interrupted and the splash jet is observed below the roof of the cavity for the first time (May, 1975). Gillbarg and Anderson (1948) are the first one, who explained the under-pressure based on the dynamic pressure term from the Bernoulli

* Corresponding author.
E-mail address: jiangyunhua211@163.com (Y. Jiang).

https://doi.org/10.1016/j.oceaneng.2018.01.091
Received 1 June 2017; Received in revised form 26 September 2017; Accepted 24 January 2018

equation and the surface tension are the chief forces make surface closure. Particularly, the ratio of the inertial force to the surface tension showing that the surface tension can be neglected in the splash crown dynamics (Gillbarg and Anderson, 1948). Later, the experimental measurement data of the cavity inner pressure shows Bernoulli pressure underestimates the true pressure differential (Abelson, 1970; Lee et al., 1997). Furthermore, the surface tension pays a role in the splash crown dynamics and cannot be neglected based on the newest experimental investigations (Marston et al., 2016). For the quantitatively, the surface closure dimensionless time $T_{sc} = t_{sc}V_0/D_c = 3.88$ is roughly constant for a sphere vertical experiments under an atmosphere pressure and constant air density (May, 1975). Where, t_{sc}, V_0, D_c, are the surface closure time, water entry velocity and the diameter of the sphere, respectively. It is worth noting that the effects of the entry angles and ventilation rates to the crown splash development and surface closure has not been examined based on the prior published works.

For the pull away, which is a phenomenon of the cavity top moving downward from the water surface and never occurs without surface closure. The pull away may not occur when the cavity pressure does not drop sufficiently (May, 1975). The pull away time is linearly increase with the entry velocity, whatever the head shapes are based on the vertical water entry experimental data (May, 1975). Moreover, the effects of the water entry angle on the pull away time can be neglected, as there is only a slight change with the entry angle under higher entry speeds between 300 and 1600 feet per second and entry angles from 45 to 70° (May, 1975).

For the deep closure, the dimensionless deep closure time $T_{dc} = t_{dc}V_0/D_c$ of a sphere undergoing vertical water entry in a single homogeneous fluid is a linear function of Fr, and the slope are 1.27 for sunflower oil (Tan et al., 2016) and 1.25 for water (Truscott and Techet, 2009), respectively, under the condition of the $Fr \le 40$. Moreover, there is another dimensionless deep closure time $\tau_{dc} = t_{dc}\sqrt{2g/D_c}$ is used, when the water entry velocity V_0 is much higher than the cavity collapse typical velocity scale $\sqrt{D_c/g}$ (Tan et al., 2016). Specifically, the dimensionless values of the deep closure are $\tau_{dc} = 1.74$ for a sphere undergoing vertical entry into water (Gillbarg and Anderson, 1948), $\tau_{dc} = 1.726 \pm 0.0688$ ($n = 118$ trials) for a sphere undergoing vertical entry into water (Truscott and Techet, 2009), $\tau_{dc} = 1.796$ for a sphere undergoing vertical entry into homogeneous sunflower oil (Tan et al., 2016) and $\tau_{dc} = 2.285 \pm 0.0653$ ($n = 47$ trials) for a disc undergoing vertical entry into water (Glasheen and Mcmahon, 1996), respectively. To the author's best knowledge, the pinch off depth only was discussed quantitatively for a sphere vertical water entry in single homogeneous sunflower oil and an oil-water multi-layer fluid (Tan et al., 2016). The pinch off depth is also a linear function of Fr, and the slope is approximately 0.72 for homogeneous sunflower oil under $Fr \le 30$ (Tan et al., 2016).

For the water entry cavity ripples, which were first mentioned by Worthington (1908) and then by Mallock (1918). There are two typical physical mechanism explanations based on the prior published works for the vertical water entry cavity ripples. The first one is the elastic of the air entrapped from the water surface based on the analysis by Semenenko (1998). The second one is the acoustic in origin, formed by the pressure perturbation of the pinch off based on the comments by Grumstrup et al. (2007). Moreover, the mechanism of the multiple pinch offs under the influence of the tank wall is the interaction of both the water tank wall and the attachment of the upper edge of the cavity (Mansoor et al., 2014). And, the two-layer system cavity ripples and the corresponding Strouhal number were discussed to confirm that the physical mechanism of the cavity ripples are not related to vortex shedding (Tan et al., 2016), which was measured and captured by using the PIV in Truscott et al. (2012). Additional, Gekle et al. (2008) noted that the capillary waves produced before pinch off can affect the dynamics of the cavity until the cavity collapse.

Therefore, the present study focuses on examining the fundamental flow characteristics involved in oblique and ventilation water entry under $Fr \le 20$, which has not been studied in the past. The current paper is structured as follows: Section 2 provides the details of the experimental methods. In Section 3, the experimental observations and the corresponding explanations of the water entry cavity flow characteristics under different entry angles and ventilation rates are reported. Finally, the conclusion of the experimental results are provided in Section 4.

2. Experimental methods

The systematic experiments were performed to investigate the near water surface cavity flow characteristics under different water entry angles and ventilation rates. We conducted the experiments in a water entry tank system that is designed and manufactured by ourselves, shown schematically in Fig. 1a. The water entry tank system consists of a water tank, a high-speed camera, a ventilation system, a model posture constraint system and a water entry model.

For the water tank, as shown in Fig. 1a, is a tempered-glass tank with dimensions of 1.2 m × 1.0 m × 1.2 m and a 15-mm thick rubber mat is placed on the bottom to prevent the test model from crashing on it. The images and videos of the water entry air cavity were captured by a Phantom V12.1 high-speed camera acquired 1000 frames s^{-1} at 800 × 600 resolution in ours experiments, which can acquire 6242 frames s^{-1} at 1280 × 800 resolution. To obtain better videos and images,

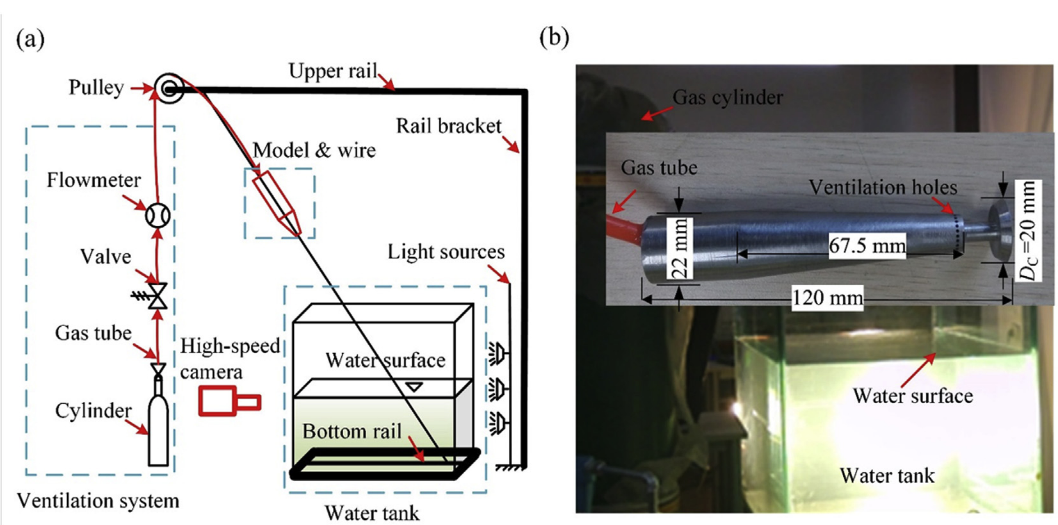

Fig. 1. (a) Schematic of the water entry tank facility. (b) Images of the test model and the water tank.